SURFACE PROPERTIES AND WETTING BEHAVIOUR
OF LIQUID Ag–Sb–Sn ALLOYS

V. Sklyarchuk[a], Yu. Plevachuk[a,*], I. Kaban[b], R. Novakovic[c]

[a] Ivan Franko National University, Department of Metal Physics, Lviv, Ukraine
[b] IFW Dresden, Institute for Complex Materials, Dresden, Germany
[c] National Research Council (CNR-IENI), Genoa, Italy

Abstract

Surface tension and density measurements of liquid Ag–Sb–Sn alloys were carried out over a wide temperature range by using the sessile drop method. The surface tension experimental data were analyzed by the Butler thermodynamic model in the regular solution approximation. The wetting characteristics of these alloys on Cu and Ni substrates have been also determined. The new experimental results were compared with the calculated values as well as with data available in the literature.

Keywords: Lead-free solders; Surface tension; Density; Contact angle; Sessile drop method; Butler's equation

1. Introduction

On implementation of the EU RoHS and WEEE directives [1] extensive investigations have been carried out to find lead-free alloys instead of traditional Pb–Sn solders. Progress has been made in the area of low-temperature lead-free solders [2], while the research is seriously lacking into replacements of Pb–Sn solder alloys, where the Pb-content is above 85 wt.%. High-temperature solders with melting temperatures above 550 K are widely used in the electronics industry for advanced packing technologies [3, 4]. Sb–Sn alloys are considered among the high-temperature solder candidates. Indeed, Sn-rich Sn–Sb alloys exhibit good electrical properties and a wide range of melting temperatures that make them appropriate in the step-soldering technology. The solders used at the early stages should be characterized by higher melting temperatures in order not to be molten during the subsequent soldering [5].

As silver is one of the main materials for the conduction lines and pads in multilayer low-temperature ceramic substrates, Sb–Sn solder joints form Ag–Sb–Sn contacts because of the dissolution and interfacial reactions. Thus, binary Sb–Sn solders with intake of Ag are transformed into the ternary Ag–Sb–Sn phases. The ternary Ag–Sb–Sn alloys are characterized by enhanced mechanical properties, fatigue resistance, and thermal resistance with respect to the eutectic Ag–Sn solder, thus rendering it suitable for use in high temperature service environments [6].

In the present work, the thermophysical properties relevant to the soldering such as density, surface tension and wetting behavior on Cu and Ni substrates for the ternary Ag–Sb–Sn liquid alloys with high Sn-content have been investigated.

2. Experimental

The density, surface tension and wetting characteristics of the $Ag_9Sb_{20}Sn_{71}$, $Ag_{7.5}Sb_{15}Sn_{77.5}$, $Ag_6Sb_{10}Sn_{84}$ and $Ag_6Sb_8Sn_{86}$ (at.%) liquid alloys have been measured over a wide temperature range above the liquidus by means of the sessile-drop technique. Applied experimental methodology and techniques presented in this paper were already described in [7]. The alloys were prepared from pure Ag, Sb and Sn (99.99%) according to the nominal composition by arc-melting under protective atmosphere of high-purity argon after preliminary evacuation of the furnace up to the rest pressure of about 0.1 Pa. Almost spherical specimens of about 3 mm in diameter were placed on polished graphite substrates for the density and surface tension measurements [7]. Before the measurements, the graphite substrates were aligned horizontally in order to provide an axis-symmetry of the liquid drop. The axis-symmetry of the sample was checked permanently during the experimental run. The shape of the sample was captured by means of a digital CCD camera [7]. Three series comprising 20 pictures each were captured during two minutes after

Dedicated to the memory of Professor Zbigniew Moser

reaching the desired temperature. The temperature was measured with a thermocouple (type K) placed right above the sample and kept stable within ± 1 K around the selected set-point. During the experiments a pressure of less than 10^{-3} Pa was maintained in the chamber [7]. Measurements of the density and surface tension were carried out by decreasing the temperature step by step from the maximum experimental temperature. Images were taken at intervals of about 25 K after a slow cooling and temperature stabilization for several minutes. In order to avoid recording of the glowing of the heater and samples, monochromatic blue background light and a suitable filter in front of the camera were applied [7].

In order to obtain the density and the surface tension data the droplet shape was acquired and subsequently analyzed. The substrate line and the profile of the sample were found automatically by dedicated evaluation software [8]. Assuming axisymmetry of a droplet, a contour function has been obtained and then integrated in order to get the volume and, finally, with the sample mass, the density, ρ.

Determination of the surface tension, σ, is based on the analysis given by Rotenberg, Boruvka and Neumann [9]. Starting from suitable assumptions on the droplet size and its surface tension, the profile line was calculated by numerical integration of the Laplace equation [7]. Taking into account systematic errors of measurement procedure and the accuracy and repeatability of profile acquisitions, the overall or total error involved in the surface tension value is estimated to be about 7 % [10].

The wetting behaviour of liquid Ag–Sb–Sn alloys in contact with Cu and Ni-substrates has been determined with the sessile drop method. The contact angle measurements have been performed for all alloy compositions ($Ag_9Sb_{20}Sn_{71}$, $Ag_{7.5}Sb_{15}Sn_{77.5}$, $Ag_6Sb_{10}Sn_{84}$ and $Ag_6Sb_8Sn_{86}$) on Cu-substrate, while in the case of Ni-substrate only $Ag_9Sb_{20}Sn_{71}$ and $Ag_6Sb_8Sn_{86}$ were tested. For determination of the contact angle, copper and nickel plates were used as substrates. Prior to the measurement, the surface of the substrate was carefully polished, cleaned with acid and rinsed with propane. In order to achieve a uniform temperature field, at the beginning of each measurement the alloy sample was kept 15 min in the furnace at the temperature of about 20 K below its melting temperature. The measurements were carried out during heating with steps of temperature between 10 and 20 K.

3. Modeling

Based on Butler's model, the surface tension of binary and ternary liquid alloys, assuming the regular solution model, can be calculated as [11]:

$$\sigma = \sigma_i + \frac{RT}{S_i} \ln \frac{X_i^s}{X_i^b} + \frac{1}{S_i} \cdot$$
$$\cdot \left[G_i^{xs,s}(T, X_{j(j=2,3)}^s) - G_i^{xs,b}(T, X_{j(j=2,3)}^b) \right], \ i=1,2,3. \quad (1)$$

where R, T, σ, S_i are the gas constant, absolute temperature, the surface tension of pure components and the surface area, respectively $G_i^{xs,s}(T, X_{j(j=2,3)}^s)$ and $G_i^{xs,b}(T, X_{j(j=2,3)}^b)$ partial excess Gibbs energies of a component i in the surface phase and in the bulk phase, respectively. Both free energies are given as functions of T and composition of the surface and bulk phase, i.e., $X_{j(j=2,3)}^s$ and $X_{j(j=2,3)}^b$.

The surface area of component i is calculated from Avogadro's number, the atomic mass and the density data [12] as follows:

$$S_i = 1.091 N_0 (\frac{M_i}{\rho_i})^{2/3} \quad (2)$$

The excess energy term of a component i can be derived from the standard thermodynamic relation, in the form:

$$G_i^{xs} = G^{xs} + \sum_{j=1}^{n} (\delta_{ij} - X_j) \frac{\partial G^{xs}}{\partial X_j} \quad (3)$$

where δ_{ij} is Kronecker's symbol.

Assuming that the free energy of the alloy is always proportional to the number of interactive contacts between neighbouring atoms, $G_i^{xs,b}$ and $G_i^{xs,s}$ can be related to the respective coordination numbers in the surface layer and the bulk phase as:

$$G_i^{xs,s}(T, X_{j(j=2,3)}^s) = \beta G_i^{xs,b}(T, X_{j(j=2,3)}^b) \quad (4)$$

where β is the ratio between the two coordination numbers, i.e. a parameter describing the reduced coordination in the liquid phase. In typical close-packed solid structures (*bcc*, *hcp*) the coordination numbers are 12 and 9 for the bulk and the surface phases, respectively, and thus $\beta = 0.75$. However, in some cases the value of β might be affected by other factors, such as the relaxation of the surface structure, and in the literature different values ranged in $0.5 \le \beta \le 0.84$ can be found [12].

In the present paper, the excess Gibbs energies of the binary subsystems of the Ag-Sb-Sn system are given in the form of Redlich-Kister polynomials, as follows:

$$^{xs}G_L^{A-B} = x_i \cdot x_j \cdot \sum_{\upsilon=0}^{n} (A_\upsilon + B_\upsilon \cdot T) \cdot (x_i - x_j)^\upsilon \quad (5)$$

The excess Gibbs energy of the Ag-Sb-Sn liquid phase is calculated combining the corresponding values of the Ag-Sn [13], the Ag-Sb [14] and the Sb-Sn [15] binary subsystems (Eq. 5) with an additional ternary contribution [14], $x_1 x_2 x_3 L_{123}$, in the form:

$$^{xs}G_L^{A-B-C} = \sum_{i,j} x_i \cdot x_j \cdot \sum_{\upsilon=0}^{n} (A_\upsilon + B_\upsilon \cdot T) \cdot (x_i - x_j)^\upsilon + x_1 x_2 x_3 L_{123} \quad (6)$$

4. Results and discussion

4.1. Surface tension of liquid Ag-Sn, Ag-Sb and Sb–Sn alloys

Thermodynamic quantities of mixing of the Ag-Sn

[13], Ag-Sb [14] and Sb–Sn [15] systems and their phase diagrams indicate that the three binaries are compound forming systems characterised by weak interactions between the constituent atoms. Accordingly, the effects of the short range order on the surface properties of the abovementioned compound forming liquid alloys are not pronounced, as it was shown in the case of liquid Sb-Sn alloys [16]. In the present study the surface tension calculations were performed for the temperature of 1073 K, at which, according to the Ag-Sn and Ag-Sb phase diagrams [17], the liquid phases of these systems exist up to 84 at.% Ag and up to 87 at.% Ag, respectively, and the values for the Ag-rich compositions refer to a supercooled liquid state. The optimized data sets of the excess Gibbs energy of mixing, G_M^{xs}, of liquid Ag-Sn [13], Ag-Sb [14] and Sb-Sn [15] alloys (Eq. 5) together with the reference surface tension data for pure components (Ag [18], Sb [19] and Sn [20]), as well as their molar volumes [12] have been used to calculate the surface tension isotherms by the Butler model in the regular solution approximation (Eq. 1). The comparison of the surface tension literature data for the liquid Ag-Sn [21-25] (Fig. 1), Ag-Sb [19] (Fig. 2) and Sb–Sn [14, 7, 26] alloys with corresponding calculated isotherms (Fig. 3) reveals a good agreement, although in some cases, different experimental methods have been used.

4.2 Experimental results: surface tension and density of liquid Ag-Sb-Sn alloys

The density and the surface tension measurements were carried out on the $Ag_9Sb_{20}Sn_{71}$, $Ag_{7.5}Sb_{15}Sn_{77.5}$, $Ag_6Sb_{10}Sn_{84}$, $Ag_6Sb_8Sn_{86}$ liquid alloys between their melting point, T_m, and 1100 K. The experimental values of the density and surface tension are plotted in Fig. 4 and Fig. 5, respectively. The density of the
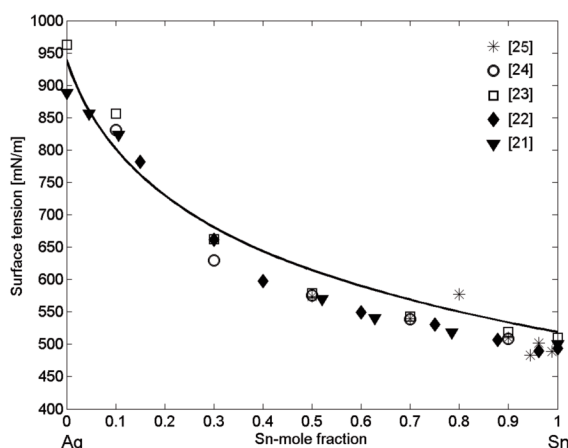

Figure 1. Surface tension isotherm (T = 1073 K) for liquid Ag-Sn alloys: line – calculation, symbols – experimental data [21-25]
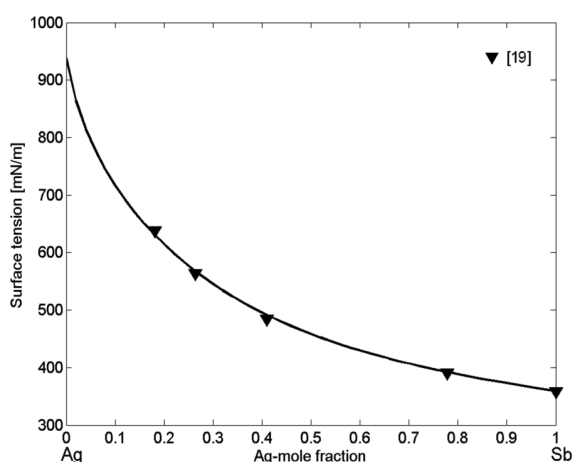

Figure 2. Surface tension isotherm (T = 1073 K) for liquid Ag-Sb alloys: line – calculation, symbols – experimental data [19].
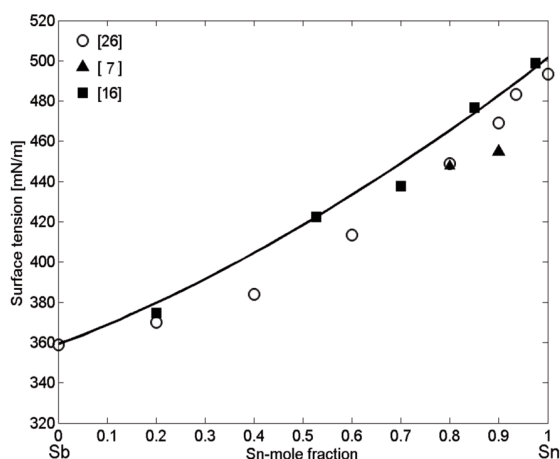

Figure 3. Surface tension isotherm (T = 1073 K) for liquid Sb-Sn alloys: line – calculation, symbols –experimental data [16, 7, 26].

Ag–Sb–Sn alloys decreases with increasing concentration of Sb from 8 at.% up to 20 at.%. Admixtures of silver from 6 to 9 at.% result in higher values of density in comparison to the density of binary Sb-Sn alloys with the same content of antimony [7, 26]. The density of the Ag–Sb–Sn alloys decreases nearly linearly with increasing temperature. In the temperature ranges investigated, the temperature dependence of the density is well described by the linear equation:

$$\rho = \rho_0 + \frac{d\rho}{dT}(T - T_m) \qquad (7)$$

where ρ_o and $\frac{d\rho}{dT}$ are the density at the melting temperature and its temperature coefficient, respectively. Parameters of the linear fits plotted in Fig. 4 are given in Table 1.

Table 1. *Density and surface tension together with the corresponding temperature coefficients of Sn-rich ternary liquid alloys of the Ag–Sb–Sn system.*

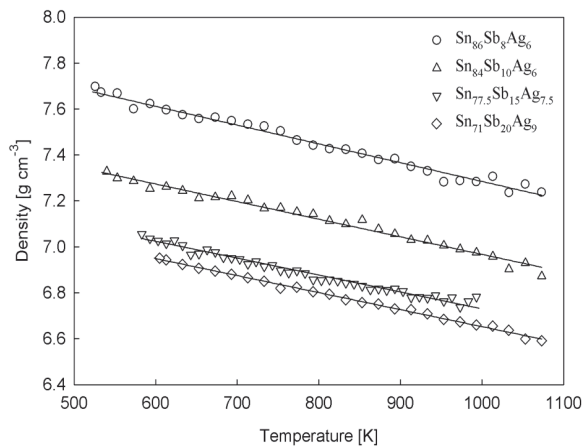| Composition [at.%]	Melting temp. / T_m [K]	Temp. range of ρ and σ-measurements [K]	Density / ρ_o at T_m [g·cm^{-3}]	Density temp. coeff. /$d\rho/dT$ [10^{-4}· g·cm^{-3}·K^{-1}]	Surface tension / σ_o at T_m [mN·m^{-1}]	Surface tension temp. coeff. / $d\sigma$ /dT [mN·m^{-1}·K^{-1}]
$Ag_6Sb_8Sn_{86}$	525	525–1100	7.67	-8.18	610	-0.07
$Ag_6Sb_{10}Sn_{84}$	540	540–1100	7.32	-7.66	613	-0.19
$Ag_{7.5}Sb_{15}Sn_{77.5}$	582	582–1100	7.04	-7.33	560	-0.08
$Ag_9Sb_{20}Sn_{71}$	605	605–1100	6.95	-7.41	502	-0.05

Figure 4. *Temperature dependence of the density for liquid Ag–Sb–Sn alloys. Lines are linear fits (please see Table 1).*
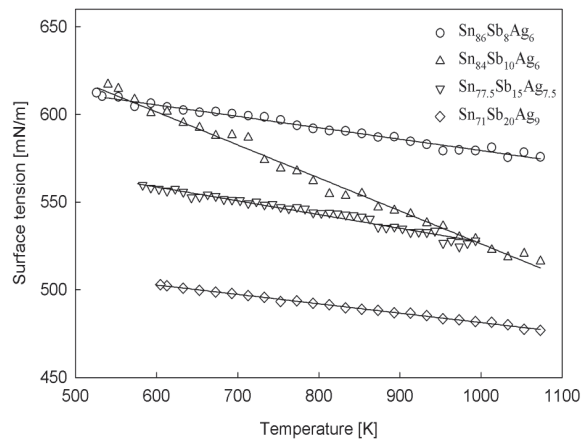

Figure 5. *Temperature dependence of the surface tension for liquid Ag–Sb–Sn alloys. Lines are linear fits (please see Table 1).*

The experimental values of the surface tension for the $Ag_9Sb_{20}Sn_{71}$, $Ag_{7.5}Sb_{15}Sn_{77.5}$, $Ag_6Sb_{10}Sn_{84}$, $Ag_6Sb_8Sn_{86}$ liquid alloys measured in this work are shown in Fig. 5. The surface tension of the Ag-Sb-Sn alloys decreases with increasing concentration of Sb from 8 at.% up to 20 at.%. The temperature dependence of the surface tension, $\sigma(T)$ is well described by the linear law (Eq. 8) with the parameters given in Table 1.

$$\sigma = \sigma_0 + \frac{d\sigma}{dT}(T - T_m) \qquad (8)$$

Here σ_o and $\frac{d\sigma}{dT}$ are the surface tension at the melting temperature and the surface tension temperature coefficient, respectively.

The density and surface tension experimental data for liquid Ag-Sb-Sn alloys have also been reported in [27]. Those data cover the temperature range of the present measurements, while the compositions are different and thus, due to the lack of literature data it was impossible to compare the new experimental data.

The surface tension for liquid Ag-Sb-Sn alloys has been calculated for $T = 1073$ K using the Butler thermodynamic model in the regular solution

approximation (Eqs. 1-4). The excess Gibbs energy of liquid Ag-Sb-Sn alloys has been calculated with Eq. (6), taking into account the energetic contributions of the binary subsystems (Eq. 5). The surface tension data obtained in the present work exhibit a good
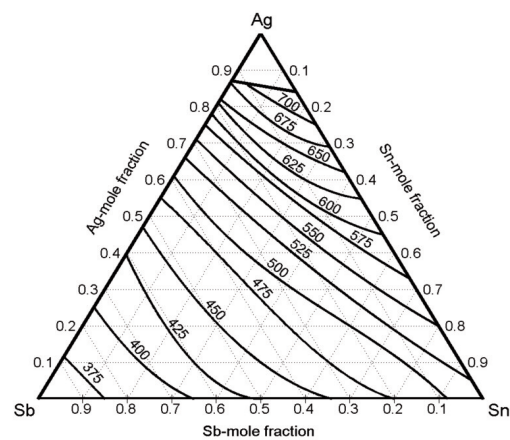

Figure 6. *Iso-surface tension lines for liquid Ag-Sb-Sn alloys calculated for T = 1073 K using the Butler model in the regular solution approximation*

agreement with the calculated values (Fig. 6). The surface tension data for liquid $Ag_{3.69}Sb_3Sn_{93.31}$, $Ag_{3.57}Sb_6Sn_{90.43}$ and $Ag_{3.46}Sb_9Sn_{87.54}$ alloys reported by Moser et al [27] agree also well with the calculated results.

4.3 Wetting

The wetting angles for the liquid $Ag_9Sb_{20}Sn_{71}$, $Ag_{7.5}Sb_{15}Sn_{77.5}$, $Ag_6Sb_{10}Sn_{84}$, $Ag_6Sb_8Sn_{86}$ alloys in contact with Cu and Ni substrates as a function of temperature are shown in Fig. 7. For each alloy, the values of the initial and final contact angle along with the corresponding temperature are given in Table 2.

Table 2. *Contact angles and temperature values for the liquid alloys/substrates studies*

Composition / at.%	Cu substrate				Ni substrate			
	θ_1/ $\degree$	T_1/K	θ_2/ $\degree$	T_2/K	θ_1/ $\degree$	T_1/K	θ_2/ $\degree$	T_2/K
$Ag_6Sb_8Sn_{86}$	100	530	33	605	137	550	62	760
$Ag_6Sb_{10}Sn_{84}$	150	545	35	683				
$Ag_{7.5}Sb_{15}Sn_{77.5}$	90	585	32	780				
$Ag_9Sb_{20}Sn_{71}$	85	608	35	740	132	605	46	770

A sharp drop of the contact angle was observed for all alloys investigated in contact with Cu substrate, while in the case of Ni substrate, its value decreases gradually with an increase in temperature to the final value. Although the Sb-content in the alloys investigated varies between 8 and 20 at.% and the Ag-content varies between 6 and 9 at.%, the final values of the contact angles on Cu-substrate converge to the value of $\theta = 33\degree$. Different contact angles were observed on Ni-substrates and these values are higher with respect to those on Cu, indicating poorer wetting
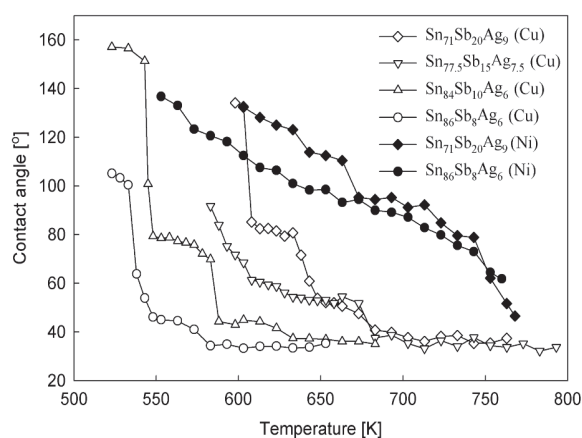
characteristics (Table 2).

Analysis of the literature data for the ternary liquid Sn-based alloys on solid Cu and Ni indicates that the wetting behaviour of Sn-rich alloys is better in the case of Cu-substrate [3, 28]. For example, it was found that the wetting of the $Ag_{3.73}Bi_{2.79}Sn_{93.48}$ alloy is much better on Cu than on Ni-substrate [28]. The contact angle values of 21.7$\degree$ on the Cu-substrate has been observed at 613 K, while the wetting angle of 41$\degree$ was on the Ni-substrate at 633 K. Similar results for other Sn-rich lead-free solders are reported in [29,30].

5. Conclusions

The density, surface tension and wetting on the Cu and Ni-substrates have been studied for the Sn-rich Ag–Sb–Sn liquid alloys in the temperature range from their melting point up to 1100 K. The experimental temperature dependences of the surface tension and density obey a linear law. The surface tension of liquid Ag–Sb–Sn alloys was calculated by the Butler model in the regular solution approximation and the computed values agree quite well with the experimental data. The Sn-rich Ag–Sb–Sn liquid alloys show better wetting behavior on Cu-substrates in comparison to that observed in the case of Ni-substrates. The wetting characteristics of the systems investigated are similar to those of other Sn-based solders described in the literature.

Figure 7. *Variations of contact angle as function of temperature for the liquid Ag–Sb–Sn alloys on Cu and Ni-substrates*

References

[1] WEEE and RoHS Directives. Official Journal of the European Union, L37, 2003, p.19.

[2] Handbook of Properties of SAC Solders and Joints. C. Schmetterer, H. Ipser, J. Pearce (Eds.), ELFNET - COST 531 Lead-Free Solders, Vol. 2). COST Office, Brussels, 2008 (ISBN 978-80-86292-26-7); http://www.univie.ac.at/cost531

[3] M. Abtew, G. Selvaduray, Mater. Sci. Eng., R 27 (2000) 95–141.

[4] F. Gayle, G. Becka, J. Badgett, G. Whitten, T. Pan, A. Grusd, B. Bauer, R. Lathrop, J. Slattery, I. Anderson, J. Foley, A. Gickler, D. Napp, J. Mather, C. Olson, JOM, 53 (2001) 17–21.

[5] S.-W. Chen, P.-Y. Chen, C.-H. Wang, J. Electron. Mater., 2006, 35(11), 1982–1885.

[6] H.-T. Lee, H.-S. Lin, C.-S. Lee, P.-W. Chen, Materials

Sci. and Eng., A407 (2005) 36–44.

[7]   Yu. Plevachuk, W. Hoyer, I. Kaban, M. Köhler, R. Novakovic, J. Mater. Sci. 45 (2010) 2051–2056.

[8]   S. Gruner, M. Köhler, W. Hoyer, J. Alloys Compd., 482 (2009) 335–338.

[9]   Y. Rotenberg, L. Boruvka, A.W. Neumann, J. Colloid Interf. Sci., 93 (1983) 169–183.

[10] Joint Committee for Guides in Metrology (JCGM/WG1), GUM 1995 with minor corrections, Evaluation of measurement data — Guide to the expression of uncertainty in measurement, First edition September 2008, Corrected version 2010, © JCGM 2008, pp. 1–120.

[11] J.A.V. Butler, Proc. Royal Soc. A135 (1932) 348–375.

[12] T. Iida, R.I.L. Guthrie, The Physical Properties of Liquid Metals, Clarendon Press, Oxford, 1993.

[13] U.R. Kattner, W. J. Boettinger, J. Electron. Mater., 23 (1994) 603–610.

[14] W. Gierlotka, Y.-C. Huang, S.-W. Chen, Metall. and Mater. Trans., 39A (2008) 3199–3209.

[15] B. Jönsson, J. Ågren, Mater. Sci. Technol., 2 (1986) 913–916.

[16] R. Novakovic, D. Giuranno, E. Ricci, S. Delsante, D. Li, G. Borzone, Surf. Sci., 605 (2011) 248–255.

[17] T.B. Massalski, P.R. Subramanian, H. Okamoto, L. Kacprzak (Eds.), 2nd Edition, Binary Alloy Phase Diagrams, Vols. 1–3, ASM, International Materials Park, OH, 1990.

[18] R. Novakovic, E. Ricci, D. Giuranno, A. Passerone, Surf. Sci., 576 (2005) 175–187.

[19] I. Lauermann, F. Sauerwald, Z. Metallkde, 55 (1964) 605–612.

[20] R. Novakovic, D. Giuranno, E. Ricci, T. Lanata, Surf. Sci. 602 (2008) 1957–1963.

[21] I. Lauermann, G. Metzger, F. Sauerwald, Z. Phys. Chem. 216 (1961) 42-49.

[22] Z. Moser, W. Gąsior, J. Pstruś, J. Phase Equil., 22 (2001) 254-258.

[23] J. Lee, W. Shimoda, T. Tanaka, Mater. Trans., 45 (2004) 2864–2870.

[24] M. Kucharski, P. Fima, Monatsh. Chem. 136 (2005) 1841–1846.

[25] P. Fima, Appl. Surf. Sci. 257 (2011) 3265–3268.

[26] W. Gąsior, Z. Moser, J. Pstruś, J. Phase Equil., 24 (2003) 504–510.

[27] Z. Moser, W. G., J. Pstrus, S. I., X.J. Liu, I. Ohnuma, R. Kainuma, K. Ishida, Mater. Trans., 45 (2004) 652–660.

[28] I. Kaban, K. Khalouk, M. Köhler, W. Hoyer, J.-G. Gasser, J. Electron. Mater. 39 (2010) 70–76.

[29] F. Gnecco, E. Ricci, S. Amore, D. Giuranno, G. Borzone, G. Zanicchi, R. Novakovic, Int. J. Adhesion & Adhesives 27 (2007) 409–416.

[30] S. Amore, E. Ricci, G. Borzone, R. Novakovic, Mater. Sci. Eng., A 495 (2008) 108–112.